Performance of Blind Turbo Equalizer in Indoor Channels

Mohamed Lassaad Ammari

Original scientific paper

***Abstract*—In this paper, we consider the transmission of turbo coded symbols in the indoor radio environment. The system is affected by the intersymbol interference (ISI) caused by the multipath time-delay spread of the transmission medium. To reduce the channel effect, we propose to use a blind turbo equalizer combining channel estimation, equalization and turbo decoding. The equalizer consists of an interference canceller (IC) and a MAP-BCJR decoder. To improve system performances, we redefine the channel reliability factor used by the MAP-BCJR decoding algorithm. We propose a new metric that takes into account the statistics of the signal at the equalizer output. The channel coefficient estimation is performed using a recursive least squares (RLS) algorithm. A blind receiver initialization technique is proposed. This technique is based on a soft decision-directed least mean square algorithm (soft DD-LMS). For the proposed turbo detector, the ISI cancellation, channel estimation and decoding are jointly performed through an iterative process where modules exchange a soft information.**

***Index Terms*—Indoor channel, MAP decoder, turbo processing, channel reliability, RLS channel estimation.**

I. Introduction

Digital communications in building environments have been widely studied in recent years [1]–[4]. They provide users the possibility to exchange information and many application files in a local area. To ensure the compatibility of wireless transmission with cabled local area networks (LAN) and to support multimedia applications, data rates on the order of 10 Mbps and more are needed [5]. It has been shown in [5], [6] that it is possible to increase considerably the transmission rate by using a DFE equalizer at the receiver. These cited articles consider M-QAM/DFE systems with uncoded symbols. In this paper, we suppose that the transmitted symbols are turbo coded and QPSK modulated. We analyze the behavior of the turbo equalization and we compare the performance of the proposed turbo detector with that of the DFE equalizer and the turbo equalizer given in [7].

Turbo codes introduced in [8] can achieve performance close to the Shannon capacity limit in both the additive white Gaussian noise channel (AWGN) and the Rayleigh flat-fading channel with perfect knowledge of the channel statistics. The iterative decoding process with extrinsic information exchange, called "turbo principle", is considered as the most important development in channel coding theory. The good performances given by turbo decoders are attributed to this turbo principle which has been used recently in several applications. In 1995, Douillard *et al*. [9] presented, for the first time, turbo equalization as an iterative process inspired from the turbo decoding principles. In fact, for turbo equalization, the ISI cancellation and decoding are jointly performed through an iterative process where each module uses the soft extrinsic information provided by the other. This technique allows for the use of all available information [10] and improves the system performance. The turbo detector proposed in [9] uses the iterative MAP algorithm for both equalization and decoding. This scheme achieves a good performance but it suffers from high complexity [10], [11]. Many researchers have proposed turbo equalizer architectures [7], [9]–[12], using different algorithms in order to reduce the computational complexity.

In this paper, we use a turbo equalizer having the same structure proposed in [7]. So, the turbo detector consists of an intersymbol interference canceller (IC) and a MAP-BCJR decoder. The IC needs the knowledge of the channel coefficients. The authors in [7] have assumed that the channel is perfectly known at the receiver. Thus, for the first iteration of the turbo equalizer, the IC is fed by zero since the symbol estimation is not available. In this paper, we consider a blind equalization and we assume that the channel state information in unknown which is a more realistic constraint. So, we have introduced a channel estimation module in our turbo detector. Thereby, we propose to use a blind equalizer at the first iteration in order to provide the symbol estimation to both the IC and the channel estimator.

Furthermore, unlike [7] where data are convolutionally coded, we use in this paper a turbo encoder. Thus, we have to redefine the channel reliability factor used by the MAP-BCJR decoding algorithm. We propose a new metric that takes into account the statistics of the signal at the IC equalizer output. The MAP decoder is also modified as in [13] in order to compute the log likelihood ratio (LLR) of both systematic and coded symbols.

The outline of this paper is as follows. In section II, the system and channel models are described. Section III presents the turbo detection principle and proposes a blind turbo detector. We also describe, in this section, the evaluation of the channel reliability factor used by the MAP-BCJR decoder. Section IV discusses the channel estimation procedure. In section V, we present simulation results for different scenarios and we compare the proposed detector with the DFE equalizer and the turbo equalizer of [7]. Finally, a conclusion is given in section VI.

Manuscript received August 16, 2010; revised February 18, and April 27, 2011.

M. L. Ammari is with 6'Tel Research Unit, School of Communications of Tunis, University of Carthage, Tunisia, (email: mlammari@ele.etsmtl.ca).

1845-6421/11/8219

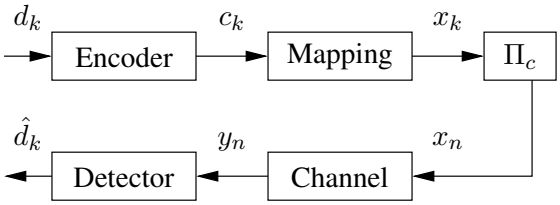

Figure 1. System and channel model.

II. System and channel model

Let us consider the baseband system model shown in Fig. 1. The information data stream $\{d_k\}$ of length L_d is encoded using an $R = 1/3$ rate turbo code to yield the coded sequence $\{c_k\}$ of length $N = L_d/R$. The coded bits are passed to the QPSK modulator. The modulated sequence $\{x_k\}$, for $k = 1, \cdots, N/2$, is then interleaved to give $\{x_n\}$ and transmitted over the indoor channel. The transmitted signal is thus:

$$u(t) = \sum_n x_n g(t - nT_s) \tag{1}$$

where $g(t)$ is the baseband pulse shape and T_s the symbol period.

The indoor radio channel is affected by the multipath propagation phenomenon caused by multiple reflections of the transmitted signal. The most common impulse response for the indoor channel model is represented by [1]:

$$h(t,\tau) = \sum_{l=0}^{L-1} \alpha_l(t) e^{j\theta_l(t)} \delta\left(\tau - \tau_l(t)\right) \tag{2}$$

where L is the number of multipath components and $\delta(\cdot)$ the Kronecker delta function. The existing indoor channel measurements suggest that the amplitudes α_l are Rayleigh distributed, the phases θ_l are uniformly distributed, and the arrival times τ_l form a Poisson process with average arrival rate λ [1]. The indoor channel is supposed to be wide sense stationary uncorrelated scattering. Hence, its autocorrelation function is given by:

$$\mathrm{E}\left\{h(t_1,\tau_1)h^*(t_2,\tau_2)\right\} = Q(t_1 - t_2, \tau_1)\delta(\tau_1 - \tau_2) \tag{3}$$

where $Q(t,\tau)$ is called the power delay profile and $*$ denotes complex conjugate. The power delay profile $Q(t,\tau)$ represents the expected received power as a function of the delay τ [5]. It has been shown that the power delay profile can take either exponential or uniform shape [5]. In this paper, we use the exponential power delay profile.

Given the channel impulse response of equation (2), we can express the received signal at the n^{th} sampling instant $t = nT_s$ as:

$$\begin{aligned} y(n) &= \sum_{l=0}^{L-1} \alpha_l(n) e^{j\theta_l(n)} u\left(n - \tau_l(n)\right) + w(n) \\ &= \sum_{l=0}^{L-1} h_{n,l} x_{n-l} + w(n) \end{aligned} \tag{4}$$

where $\mathbf{h}_n = [h_{0,n}, h_{0,n}, \ldots, h_{M-1,n}]^H$ represents the channel impulse response at the sampling instant $t = nT_s$ and $w(n)$ is a zero mean AWGN with variance σ_w^2.

III. Turbo detection: joint equalization and decoding

A. Channel equalization

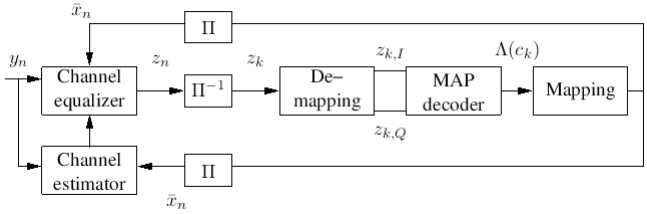

Figure 2. Turbo detector architecture.

As it is shown in (4), the received signal is affected by the ISI. Thus, the use of an equalizer at the receiver is needed. The detector is then composed of an equalizer and a MAP-BCJR decoder as in Figure 2. For turbo detection, these modules perform jointly and exchange a soft information. This approach, proposed in [9], allows for the use of the all available information and improves the system performance. Among the various turbo detector architectures, the turbo equalizer using soft ISI cancellation [7] is characterized by its good performance and its low complexity [11]. So, in this paper, we consider the (IC) equalizer composed of the two following filters [7]:

$$\begin{aligned} P(f,n) &= \beta \frac{H^*(f,n)}{E_h} \\ Q(f,n) &= \beta\left(\frac{|H(f,n)|^2}{E_h} - 1\right) \end{aligned} \tag{5}$$

where $H(f,n)$ is the time varying channel transfer function at the sampling instant $t = nT_s$, E_h is its average power and β is given by:

$$\beta = \frac{\sigma_d^2}{\sigma_d^2 + \sigma_w^2} \tag{6}$$

in which σ_d represents the data standard deviation. To compute the equalizer filters coefficients, we need to know of the channel impulse response. So, we have to estimate this response. Filters $P(\cdot)$ and $Q(\cdot)$ are then constructed using the estimated channel response and not the real one. The channel estimation technique is discussed in section IV.

The input of the matched filter $P(\cdot)$ is the sampled channel output y_n. At each iteration $(p > 1)$, the filter $Q(\cdot)$ is fed by a soft decision on the transmitted symbol x_n denoted by $\bar{x}_n^{(p-1)}$. Knowing that the sequence $\{x_n\}$ is an interleaved version of $\{x_k\}$, we have $x_n^{(p-1)} = \Pi[x_k^{(p-1)}]$. The soft information $\bar{x}_n^{(p-1)}$ is computed using the decoder output at iteration $(p-1)$ as it will be discussed in section III-C.

It was shown in [7] that under the assumption $\bar{x}_n^{(p-1)} = x_n$, the equalizer output is:

$$\begin{aligned} z_n &= \frac{\sigma_d^2}{\sigma_d^2 + \sigma_w^2}\left[x_n + \sum_{k=0}^{M-1} h_{k,n}^* w_{n+k}\right] \\ &= \beta x_n + b_n \end{aligned} \tag{7}$$

where b_n is a zero mean Gaussian noise with variance:

$$\sigma_b^2 = \beta^2 \sigma_w^2 \sum_{k=0}^{M-1} |h_{n,k}|^2 \tag{8}$$

B. First iteration processing

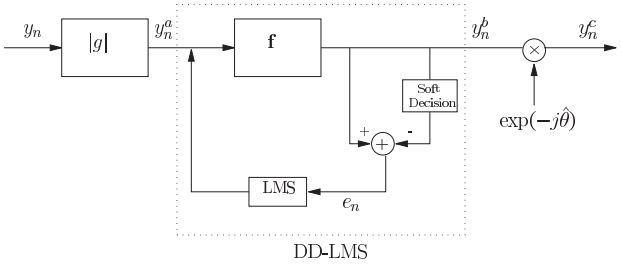

Figure 3. Structure of the blind equalizer used in the first iteration.

For the first iteration, $\bar{x}_n^{(p-1)}$ is not accessible, so we propose to use the blind equalizer structure shown in Figure 3. This equalizer is formed by the cascade of an automatic gain control (AGC), a soft decision-directed least mean square algorithm (soft DD-LMS) and a phase rotator (PR). The purpose of the AGC is to equalize the power of the received signal with that of the transmitted sequence. The AGC is a one-coefficient filter having the following output:

$$y_n^a = g_n y_n \tag{9}$$

To update the AGC coefficient, we use the adaptive algorithm given by:

$$\begin{aligned} G_n &= G_{n-1} + \mu_G \left[\sigma_d^2 - |y_n^a|^2\right] \\ g_n &= \sqrt{|G_n|} \end{aligned} \tag{10}$$

where μ_G is a positive step size and $G(0) = 1$.

The Soft DD-LMS algorithm has been introduced by [14] and is based on the classification approach used in the neural networks. This blind equalizer uses the Gaussian cluster formation algorithm [14], [15] where the cluster centers are the baseband symbols themselves. The equalization technique does not need a training sequence and consists a filtering process. Let us denote $\mathbf{f}_n$ the $(2N_s + 1)$ coefficients filter. The soft DD-LMS equalizer output is then:

$$y_n^b = \mathbf{f}_n^H \mathbf{y}_n^a \tag{11}$$

where $\mathbf{y}_n^a = [y_{n+N_s}^a, \ldots, y_{n-N_s}^a]$ and H is the Hermitian transpose. Filter coefficients are updated in order to minimize the following function [14]:

$$J(\mathbf{f}_n) = J(\mathbf{f}_{n,I}, \mathbf{f}_{n,Q}) = E\left\{\Psi(y_n^b)\right\} = E\left\{\mathbf{f}_n^H \mathbf{y}_n^a\right\} \tag{12}$$

where $\mathbf{f}_{n,I}$ and $\mathbf{f}_{n,Q}$ are the real and imaginary parts of $\mathbf{f}_n$ and $\Psi(y_n^b)$ is defined in [16] by:

$$\Psi(y_n^b) = -\log\left[f_y(y_n^b)\right] \tag{13}$$

where $f_y(y_n^b)$ is the joint Gaussian mixture distribution of the equalized signal.

For a QPSK constellation, the joint Gaussian mixture distribution of the equalized signal is [16]:

$$f_y(y_n^b) = \frac{p_m}{2\pi\sigma_{I_m}\sigma_{Q_m}} \sum_{m=1}^{4} \exp\left[-\frac{(y_{n,I}^b - \mu_{I_m})^2}{2\sigma_{I_m}^2} - \frac{(y_{n,Q}^b - \mu_{Q_m})^2}{2\sigma_{Q_m}^2}\right] \tag{14}$$

where p_m is the proportion of the m-th cluster in the mixture and $(\mu_{I_m}, \sigma_{I_m}^2)$ and $(\mu_{Q_n}^2, \sigma_{Q_n}^2)$ are the mean and variance pairs for the real and imaginary parts of the equalized symbol corresponding to a cluster m. We can impose the same variance σ_0^2 for each cluster. Furthermore, for a QPSK modulation the p_m values are taken as equal since the transmitted symbols are chosen equally likely. With these assumptions, we can update $\mathbf{f}_n$ using the classical stochastic gradient method

$$\begin{aligned} \mathbf{f}_{n+1,I} &= \mathbf{f}_{n,I} - \alpha_I \frac{\partial J(\mathbf{f}_{n,I}, \mathbf{f}_{n,Q})}{\partial \mathbf{f}_{n,I}} \\ \mathbf{f}_{n+1,Q} &= \mathbf{f}_{n,I} - \alpha_Q \frac{\partial J(\mathbf{f}_{n,I}, \mathbf{f}_{n,Q})}{\partial \mathbf{f}_{n,Q}} \end{aligned} \tag{15}$$

where α_I and α_Q are the step size parameters.

The partial derivatives can be written as [16]:

$$\begin{aligned} \frac{\partial J(\mathbf{f}_{n,I}, \mathbf{f}_{n,Q})}{\partial \mathbf{f}_{n,I}} &= \frac{1}{\sigma_0^2}\left[\left(y_{n,I}^b - \sigma_d \frac{e^{2\sigma_d y_{n,I}^b/\sigma_0^2} - 1}{e^{2\sigma_d y_{n,I}^b/\sigma_0^2} + 1}\right)\right] \\ &\quad + \frac{1}{\sigma_0^2}\left[\left(y_{n,Q}^b - \sigma_d \frac{e^{2\sigma_d y_{n,Q}^b/\sigma_0^2} - 1}{e^{2\sigma_d y_{n,Q}^b/\sigma_0^2} + 1}\right)\right] \end{aligned} \tag{16}$$

and

$$\begin{aligned} \frac{\partial J(\mathbf{f}_{n,I}, \mathbf{f}_{n,Q})}{\partial \mathbf{f}_{n,Q}} &= \frac{1}{\sigma_0^2}\left[\left(y_{n,I}^b - \sigma_d \frac{e^{2\sigma_d y_{n,I}^b/\sigma_0^2} - 1}{e^{2\sigma_d y_{n,I}^b/\sigma_0^2} + 1}\right)\right] \\ &\quad - \frac{1}{\sigma_0^2}\left[\left(y_{n,Q}^b - \sigma_d \frac{e^{2\sigma_d y_{n,Q}^b/\sigma_0^2} - 1}{e^{2\sigma_d y_{n,Q}^b/\sigma_0^2} + 1}\right)\right] \end{aligned} \tag{17}$$

The phase rotator (PR) is often necessary to correct the phase error between the transmitted and the received signal. This procedure consists of a multiplication of the signal y_n^b by $e^{-j\hat{\theta}(n-1)}$, where $\hat{\theta}(n)$ is an estimate of the phase error. The (PR) process is given in [17] by:

$$y_n^c = y_n^b \exp[-j\hat{\theta}(n-1)] \tag{18}$$

$$\hat{\theta}(n) = \hat{\theta}(n-1) + \mu_\theta \left(\epsilon(n) + \beta_\theta \sum_{k=1}^{n} \epsilon(k)\right) \tag{19}$$

$$\epsilon(k) = Im\left\{y_n^c[\hat{x}_n - y_n^c]^*\right\} \tag{20}$$

where μ_θ is a small positive step size, $\hat{\theta}(0) = 0$ and $\hat{x}_n$ is the estimate of x_n. Once y_n^c is evaluated, it is passed to the IC equalizer and to the channel estimator who consider y_n^c as a soft decision on x_n.

C. De-Mapping, MAP decoding and Mapping

The decoder uses a soft information about all coded bits to provide their LLR. Thus, a de-mapping function is necessary to convert the complex sequence at the equalizer output to real stream. The inphase (I) and the quadrature (Q) parts of the equalized symbol $z_n = z_{n,I} + iz_{n,Q}$ are decoupled and

arranged. For QPSK modulation, each modulated symbol x_k represents two bits c_{2k-1} and c_{2k} for $k = 1, \cdots N/2$. At the receiver, the de-mapping function decouples the (I) and (Q) parts of the equalized symbols. Therefore, the decoder input is $\mathbf{r} = [r_1, \ldots, r_N] = [z_{1,I}, z_{1,Q}, \ldots, z_{N,I}, z_{N,Q}]$.

Using the sequence $\mathbf{r}$, the decoder evaluates the LLR of both systematic and coded symbols defined as:

$$\Lambda(c_n) = \ln\left\{\frac{\Pr(c_n = +1|\mathbf{r})}{\Pr(c_n = -1|\mathbf{r})}\right\} \tag{21}$$

The decoding process consists of the MAP-BCJR algorithm presented in [8]. However, we have to consider the statistics of the equalizer output and recalculate the channel reliability factor. This metric can be estimated using the conditional probability density function of the decision variable z_n at the IC equalizer output $\mathrm{p}(z_n|x_n)$. We note that $\mathrm{p}(z_n|x_n)$ can be expressed as $\mathrm{p}(z_n|x_n) = \mathrm{p}(z_{n,I}|x_{n,I})\,\mathrm{p}(z_{n,Q}|x_{n,Q})$, where we have:

$$\mathrm{p}(z_{n,I}|x_{n,I}) = \frac{1}{\sqrt{2\pi}\sigma_b^2}\exp\left(-\frac{|z_{n,I} - \beta x_{n,I}|^2}{2\sigma_b^2}\right) \tag{22}$$

Substitution of $z_{n,I}$ and $x_{n,I}$ by $z_{n,Q}$ and $x_{n,Q}$ into relation (22) gives $\mathrm{p}(z_{n,Q}|x_{n,Q})$. Using the equation (22), we can write:

$$\ln\left\{\frac{\mathrm{p}(z_{n,I}|x_{n,I} = +1)}{\mathrm{p}(z_{n,I}|x_{n,I} = -1)}\right\} = \frac{2\beta}{\sigma_b^2}z_{n,I}, \quad n = 1, \cdots, \frac{N}{2} \tag{23}$$

which yields to:

$$\ln\left\{\frac{\mathrm{p}(c_n|r_n = +1)}{\mathrm{p}(c_n|r_n = -1)}\right\} = \frac{2\beta}{\sigma_b^2}r_n, \text{ for } n = 1, \cdots, N \tag{24}$$

So the channel reliability factor is:

$$L_n^c = \frac{2\beta}{\sigma_b^2} = 2\left[\beta\,\sigma_w^2\sum_{k=0}^{M-1}|h_{n,k}|^2\right]^{-1} \tag{25}$$

In the next section, we compare the performance achieved by the use of L_c given by (25) and that given by the conventional metric. We recall that the conventional definition of L_c is $2/\sigma_n^2$. It is noted that for a small value of σ_n^2, we have $\beta \approx 1$. So, if we consider that the channel coefficients $h_{n,k}$ are normalized, ie,

$$\sum_{k=0}^{M-1}|h_{n,k}|^2 = 1, \qquad \forall n \in \{1, \ldots, N\} \tag{26}$$

the channel reliability of (25) becomes $L_n^c \approx 2/\sigma_w^2$. This L_n^c expression is the same for an AWGN channel. In fact, under the above assumptions, the signal to noise ratio (SNR) at the equalizer output is identical to the SNR at the output of AWGN without ISI [7] and the interferences are canceled. However, the relation (26) is generally not satisfied.

The LLR at the decoder output are used to evaluate the soft symbol (modulated) estimates, which are needed by the IC equalizer and the channel estimator. Since each QPSK symbol ($x_k = c_{2k-1} + ic_{2k}$) is associated with two bits, the soft estimation of the modulated symbol, at iteration (p) is given by $\bar{x}_k = \bar{c}_{2k-1} + i\bar{c}_{2k}$, where:

$$\bar{c}_l^{(p)} = \mathrm{E}\left[c_l^{(p)}\right] = \tanh\left[\frac{\Lambda(c_l)}{2}\right], \quad l = 1, \cdots, N \tag{27}$$

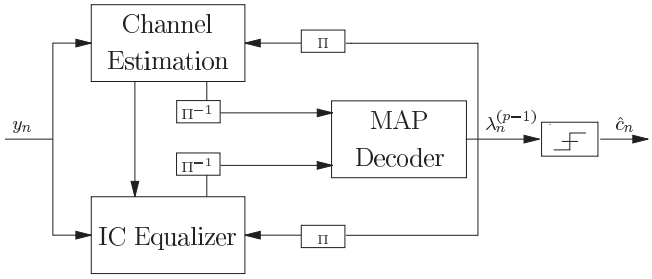

Figure 4. Global receiver architecture.

where $\Lambda(c_l)$ is the LLR of c_l delivered by the the decoder at iteration (p).

IV. Channel estimation

As we have seen above, the IC equalizer needs the knowledge of the channel impulse response. So, the estimation of this response is required. Because the indoor channel is a time-varying one, we propose to use the recursive least square (RLS) algorithm to estimate the channel response

$$\mathbf{h}_n = (h_{n,0}, h_{n,1}, \cdots, h_{n,M-1}) \tag{28}$$

This algorithm, known for its fast tracking ability, is often used for the time-varying channel estimation. The RLS algorithm is a least square technique minimizing the cost function [18], [19]

$$J(n) = \sum_{k=0}^{n}\varepsilon^{n-k}|y_k - \hat{\mathbf{h}}_k^H\bar{\mathbf{x}}_k|^2 \tag{29}$$

where $0 < \varepsilon \leq 1$ is the forgetting factor of the algorithm and $\bar{\mathbf{x}}_k = [\bar{x}_k, \bar{x}_{k-1}, \ldots, \bar{x}_{k-M}]$ represents the soft estimated value of x_k at the iteration $(p-1)$. The cost function of (29) is minimized by the following algorithm

$$\begin{aligned}
\hat{\mathbf{h}}_{k+1} &= \hat{\mathbf{h}}_k + K_k(y_k - \bar{\mathbf{x}}_k\hat{\mathbf{h}}_k)\\
\mathbf{K}_k &= \mathbf{P}_k\bar{\mathbf{x}}_k^t\mathbf{R}_k^{-1}\\
\mathbf{R}_k &= \bar{\mathbf{x}}_k\mathbf{P}_k\bar{\mathbf{x}}_k^t + \varepsilon\\
\mathbf{P}_{k+1} &= \varepsilon^{-1}(\mathbf{P}_k - \mathbf{K}_k\bar{\mathbf{x}}_k\mathbf{P}_k)
\end{aligned} \tag{30}$$

where $\mathbf{K}_k$ is the Kalman gain vector and $\mathbf{P}_k$ the error covariance matrix of channel state estimates [18], [19]. For initialization, we use $\mathbf{P}_0 = \delta_{RLS}\mathbf{I}_L$, where δ_{RLS} is a small positive real number and $\mathbf{I}_L$ denotes the $L \times L$ identity matrix. The starting estimator $\hat{\mathbf{h}}_{-1}$ is taken as the all zero vector [20].

We note that the effectiveness of the proposed channel estimation technique depends on the successfulness of the turbo equalizer. This estimator module is coupled with the turbo detector presented above. The global receiver is then given by the diagram of Figure 4. We can see that the estimated channel coefficients at iteration (p) are fed to the IC equalizer and the MAP decoder. Theses components use this information to update the equalizer parameters and to perform the decoding process. Even though the detector does not use a training sequence, we show, in the next section, that the iterative detection converges and allows for channel estimation and data decoding.

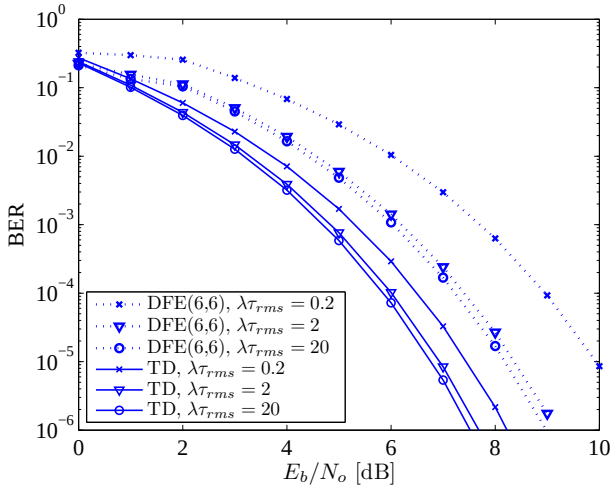

Figure 5. BER comparison of turbo detector and DFE(6,6) equalizer for different values of $\lambda\tau_{rms}$. The normalized data rate is $R_b\tau_{rms} = 0.1$.

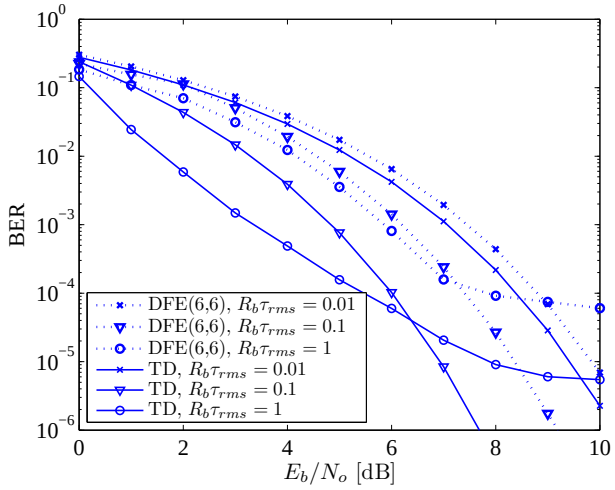

Figure 6. BER comparison of turbo detector and DFE(6,6) equalizer for different values of $R_b\tau_{rms}$. The normalized arrival rate is $\lambda\tau_{rms} = 2$.

V. Simulation Study

This section examines the effectiveness of the proposed turbo detector and compares its performance with that of the classical DFE equalizer and the turbo equalizer (TE) of [7]. In our simulations, we have considered the Saleh-Valenzuela indoor channel [1]–[3] described in section II with different normalized arrival rates $\lambda\tau_{rms}$ and normalized data rates $R_b\tau_{rms}$ (τ_{rms} denotes the *rms* multipath spread).

For the channel coding, we have considered a turbo code with a nominal code rate $1/3$, a constraint length $K = 3$ and a generator matrix $(1, 5/7)$ in octal form. The data frame size was $L = 1024$ bits. In order to reduce the burst error, we have used a block interleaver of size 32×32. The turbo detector has been iterated 6 times.

For the RLS algorithm, the forgetting factor has been fixed to $\varepsilon = 0.95$. At the first iteration, we have used the following parameters

- AGC step size : $\mu_G = 10^{-2}$
- DD-LMS step size : $\mu_f = 5 \times 10^{-4}$
- DD-LMS filter size : $2M + 1 = 11$
- Phase rotator parameters : $\mu_\theta = 0.02$ and $\beta_\theta = 0.04$

It is also noted that the simulated DFE(6,6) equalizer has six forward and six feedback taps.

Figure 5 compares the BER performance of the proposed turbo detector (TD) and the DFE equalizer for a normalized data rate $R_b\tau_{rms} = 0.1$ and for different values of $\lambda\tau_{rms}$. We can see that the performance of both DFE and turbo detector increases as $\lambda\tau_{rms}$ increases. However, for $\lambda\tau_{rms} > 2$, the difference is insignificant. When the DFE equalizer is used, we note a difference of 1.6 dB at a BER of 10^{-4} between performance achieved for $\lambda\tau_{rms} = 0.2$ and $\lambda\tau_{rms} = 20$. For the turbo detector, this difference is less than 0.7 dB.

As it is shown in Figure 5, the proposed detector improves the BER performance. For $\lambda\tau_{rms} = 0.2$, the gain of the turbo detector over the DFE equalizer is about 2.4 dB at a BER of 10^{-4}. This improvement is less substantial when $\lambda\tau_{rms}$ increases. Figure 6 shows the BER performance of

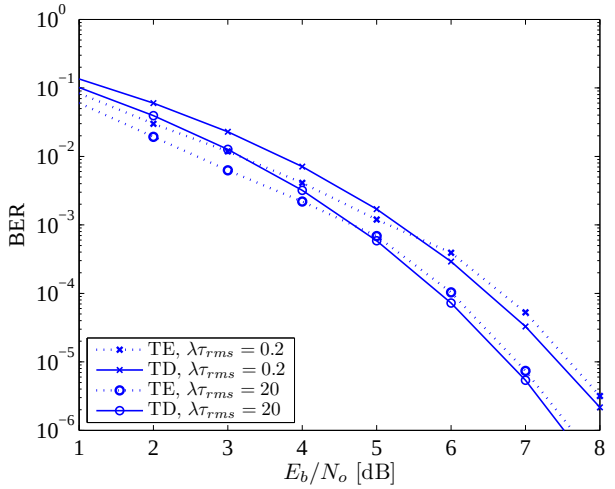

Figure 7. BER comparison of turbo detector and turbo equalizer of [7] for different values of $\lambda\tau_{rms}$. The normalized data rate is $R_b\tau_{rms} = 0.1$.

simulated systems for various normalized data rate $R_b\tau_{rms}$. The normalized arrival rate is fixed to $\lambda\tau_{rms} = 2$. For both DFE and turbo equalizers, performances are better when $R_b\tau_{rms}$ increases from 0.01 to 0.1. However, for high value $R_b\tau_{rms} = 1$, we observe a performance degradation at high SNR values represented by an irreducible residual ISI. This result is coherent with Sexton *et al.* [1]. We can see that for all simulated normalized data rates, the proposed equalizer works better than the DFE equalizer. However, the gain achieved by the turbo equalizer is less important for low data rate $R_b\tau_{rms} = 0.01$. In this case, the gain is about 0.4 dB at a BER of 10^{-4}. When $R_b\tau_{rms}$ increases to 0.1, the gain becomes 1.5 dB for the same BER.

Figure 7 compares the BER performance of the proposed turbo detector (TD) with the turbo equalizer (TE) of [7]. For the TE scenario, we assume that the channel coefficients are known at the receiver and the estimated symbols are equal to

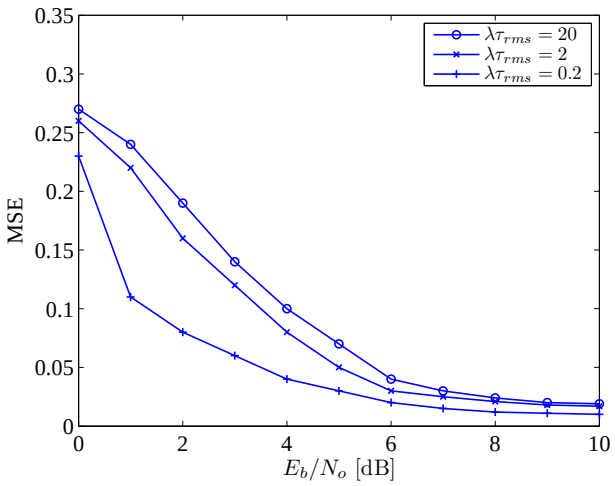

Figure 8. Performance of MMSE channel estimation.

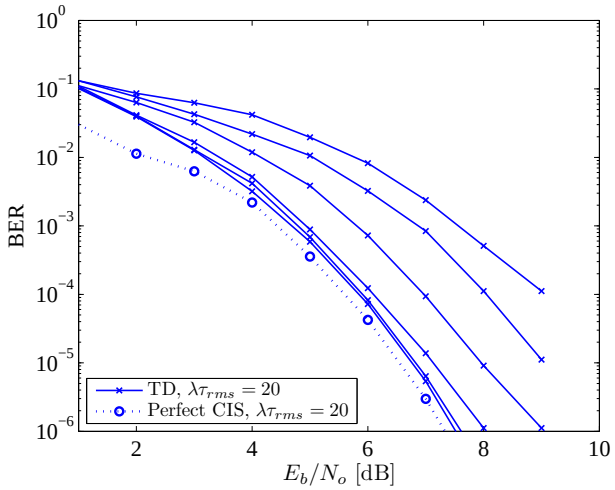

Figure 9. BER performance through the iteration process. The normalized data rate is $R_b\tau_{rms} = 0.1$.

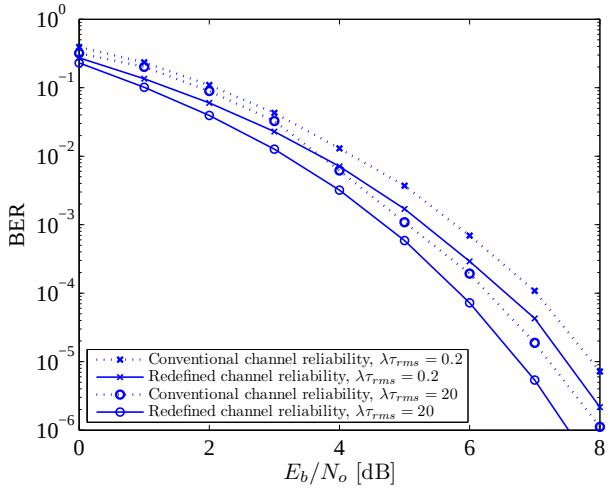

Figure 10. Effect of channel reliability factor on the BER performance. The normalized data rate is $R_b\tau_{rms} = 0.1$.

zero [7]. As we can see, when the E_b/N_o is less than 5 dB, the TE of [7] outperforms our turbo equalizer since it uses the perfect channel state information (CIS). However, when the E_b/N_o is greater than 5 dB, the channel estimation is enough accurate and the proposed TD slightly outperforms (gain of 0.1 dB) the TE of [7] since it is better initialized.

Despite the fact that the proposed TD uses a noisy channel state information (CSI), its BER performance closely matches that of the TE which assumes the perfect knowledge of channel coefficients. We can conclude that the proposed turbo detector improves the BER performance. It allows us to perform the blind equalization and the turbo decoding. The effectiveness of the turbo detector is also demonstrated by the small mean square error (MSE) of the channel estimation as shown in Figure 8.

Figure 9 illustrates the BER performance after each iteration for $R_b\tau_{rms} = 0.1$ and $\lambda\tau_{rms} = 20$. The performance of the system with the perfect channel state information (CSI) is also included in this figure to serve as a benchmark. The dotted curve corresponds to the ideal case with a perfect CSI and where the IC is fed by the true transmitted symbols. We can see a very important improvement in the BER from the first iteration to the fifth one. However, after the fifth iteration, the BER improvement is not noticeable. Furthermore, the BER curve obtained by the TD after the sixth iteration approaches that of the ideal case. Indeed the discrepancy between the two curves is about 0.2 db for a BER of 10^{-5}.

Figure 10 proves the importance of the channel reliability factor. The solid and dotted curves correspond to the BER performance obtained respectively by the redefined channel reliability (eq. 25) and the classical expression of this metric ($L_c = 2/\sigma_n^2$). We can see that the use of the redefined channel reliability factor improves the BER performance. When $\lambda\tau_{rms} = 20$, the gain obtained by the new expression is about 0.5 dB for a BER of 10^{-4}.

VI. Conclusion

The performance of a blind turbo detector in indoor channels has been evaluated for different values of normalized data rate and normalized arrival rate. The proposed blind turbo detector is an iterative process combining channel estimation, equalization and turbo decoding. The channel equalizer consists of intersymbol interference canceller filters and the turbo decoding is performed using the MAP-BCJR algorithm. We have shown, in this paper, how to redefine the channel reliability factor used by the MAP-BCJR decoder. The channel estimation is done by the RLS algorithm. To initialize the turbo detector process, we have suggested to use a blind equalizer formed by an AGC module, a soft DD-LMS algorithm and a phase rotator. At the first iteration, the channel estimator and the IC equalizer use the signal at the phase rotator output as a soft decision on the transmitted symbols. Simulation results show that the turbo detector performances are better than those of the DFE equalizer. However, the improvement achieved by the turbo detector is less important when the arrival rate

increases or the data rate decreases. The BER performance of the blind proposed TD closely matches that of the TE of [7] which assumes the perfect knowledge of channel coefficients.

REFERENCES

[1] T. A. Sexton and K. Pahlavan, "Channel modeling and adaptive equalization of indoor radio channels," *IEEE J. Select. Areas Commun.*, vol. 7, no. 1, pp. 114–121, Jan. 1989.

[2] J. L. Valenzuela, A. Valdovinos, and F. J. Casadevall, "Performance of blind equalization with higher order statistics in indoor radio environments," *IEEE Trans. Veh. Technol.*, vol. 46, no. 2, pp. 369 –374, May 1997.

[3] A. Saleh and R. Valenzuela, "A statistical model for indoor multipath propagation," *IEEE J. Select. Areas Commun.*, vol. 5, no. 2, pp. 128–137, Feb. 1987.

[4] L. J. Greenstein, S. S. Ghassemzadeh, S.-C. Hong, and V. Tarokh, "Comparison study of UWB indoor channel models," *IEEE Trans. Wireless Commun.*, vol. 6, no. 1, pp. 128–135, Jan. 2007.

[5] K. Pahlavan, S. J. Howard, and T. A. Sexton, "Decision feedback equalization of the indoor radio channel," *IEEE Trans. Commun.*, vol. 41, no. 1, pp. 164–170, Jan. 1993.

[6] J. Tellado-Mourelo, E. K. Wesel, and J. M. Cioffi, "Adaptive DFE for GMSK in indoor radio channels," *IEEE J. Select. Areas Commun.*, vol. 14, no. 3, pp. 492 –501, Apr. 1996.

[7] C. Laot, A. Glavieux, and J. Labat, "Turbo Equalization: Adative Equalization and Channel Decoding Jointly Optimized ," *IEEE J. Select. Areas Commun.*, vol. 19, no. 9, pp. 1744–1752, Sept. 2001.

[8] C. Berrou, A. Glavieux, and P. Thitimajshima, "Near Shannon limit error correcting coding and decoding: Turbo-codes," in *Proc., IEEE Int. Conf. on Commun.*, vol. 2, 1993, pp. 1064–1070.

[9] C. Douillard, M. Jézéquel, C. Berrou, A. Picart, P. Didier, and A. Glavieux, "Iterative correction of intersymbol interference: Turbo equalization," *European Transactions on Telecommunications*, vol. 6, pp. 507–511, sep/oct 1995.

[10] A. Roumy, I. Fijalkow, and D. Pirez, "Joint equalization and decoding : why choose the iterative solution? ," in *Proc., IEEE Veh. Technol. Conf.*, vol. 5, 1999, pp. 2989 –2993.

[11] M. Tüchler, R. Köetter, and A. Singer, "Turbo equalization: principles and new results," *IEEE Trans. Commun.*, vol. 50, no. 5, pp. 754–767, May 2002.

[12] M. Tüchler and A. C. Singer, "Turbo equalization: An overview," *IEEE Trans. Inform. Theory*, vol. 57, no. 2, pp. 920–951, Feb. 2011.

[13] N. D. Doan and R. M. A. P. Rajatheva, "Turbo equalization for non-binary coded modulation schemes over frequency selective fading channels," in *Proc., IEEE Veh. Technol. Conf.*, vol. 3, Tokyo, 2000, pp. 2217 –2221.

[14] J. Karaoguz and S. Ardalan, "A soft decision-directed blind equalization algorithm applied to equalization of mobile communications channels," in *Proc., IEEE Int. Conf. on Commun.*, vol. 3, 1992, pp. 1272–1276.

[15] F. Lehmann, "A Gaussian Mixture Approach to Blind Equalization of Block-Oriented Wireless Communications," *EURASIP Journal on Advances in Signal Processing*, vol. 2010, no. 1, pp. 1–10, Sept. 2010.

[16] S. J. Nowlan and G. E. Hinton, "A soft decision-directed LMS algorithm for blind equalization," *IEEE Trans. Commun.*, vol. 41, no. 2, pp. 275 –279, Feb. 1993.

[17] J. Labat, O. Macchi, and C. Laot, "Adaptive decision feedback equalization: can you skip the training period?" *IEEE Trans. Commun.*, vol. 46, no. 7, pp. 921 –930, July 1998.

[18] K. Fukawa and H. Suzuki, "Adaptive equalization with RLS-MLSE for frequency-selective fast fading mobile radio channels ," in *Proc., IEEE Global Telecomm. Conf.*, vol. 1, 1991, pp. 548 –552.

[19] M. J. Omidi, S. Pasupathy, and P. G. Gulak, "Joint data and Kalman estimation of fading channel using a generalized Viterbi algorithm," in *Proc., IEEE Int. Conf. on Commun.*, vol. 2, 1996, pp. 1198 –1203.

[20] R. Schober and W. H. Gerstacker, "Noncoherent adaptive channel identification algorithms for noncoherent sequence estimation," *IEEE Trans. Commun.*, vol. 49, no. 2, pp. 229–234, Feb. 2001.

Mohamed Lassaad Ammari received the Engineering degree from the École Supérieure des Communications, Tunis, Tunisia, in 1995, and the M.Sc. and Ph.D. Degrees from the Université Laval, Québec, QC, Canada, in 2000 and 2003, respectively. From 2003 to 2010, he was a Research Associate with the Laboratory of Communications and Integrated Microelectronics (LACIME), École de Technologie Supérieure, Montreal, QC, Canada. He is currently an Assistant Professor at the École Nationale d'Ingénieurs de Sousse. His research interests include channel equalization, OFDM systems, turbo detection and adaptive modulation.